A Two-dimensional HLLE Riemann Solver and Associated Godunov-Type Difference Scheme for Gas Dynamics

Burton Wendroff *

Abstract

The approximate three-state Riemann solver HLLE is formally extended to a nine-state two dimensional solver. The associated Godunov scheme is outlined and applied to two test problems.

1 Introduction

The purpose of this paper is to develop a two-dimensional (2D) version of the three-state HLLE Riemann solver and a corresponding Godunov method. In order to establish the notation, we begin with a review of the classical Godunov method in one dimension (1D) following [1]. In section 1.2, still following [1], we review the HLLE Riemann solver and the HLLE-Godunov scheme. In section 2 we show what Godunov's method in 2D would be if one could solve 2D Riemann problems exactly. We then present a nine-state 2D version of HLLE in section 2.1. We did this for the four-quadrant Riemann problem, but in principle this could be done for other configurations. The associated Godunov scheme is outlined, and then some computational details are described in section 2.2. In section 3 we present the result of two calculations, namely, cases 3 and 4 from [2]. These are four-shock configurations and were chosen simply to show that our 2D HLLE scheme is consistent with the solution of these problems obtained by more accurate means.

1.1 Godunov's method

In [1] B. Einfeldt gives a very lucid presentation of the original Godunov method. We wish to follow Einfeldt's notation, and so we repeat the main points here. We consider the system of conservation laws

$$v_t + f_x(v) = 0,$$

where

$$v = \begin{pmatrix} \rho \\ m \\ E \end{pmatrix},$$

*Group T-7, Los Alamos National Laboratory, Los Alamos, NM 87544, USA, (bbw@lanl.gov, http://math.unm.edu/~bbw). Work supported by the CHAMMP Program of the US Department of Energy.

and

$$f(v) = \begin{pmatrix} m \\ \frac{m^2}{\rho} + p \\ \frac{m}{\rho}(E+p) \end{pmatrix}.$$

The gas dynamic state consists of the density ρ, the velocity u, and internal energy density e. Then $m = \rho u$, $E = \rho(e + .5u^2)$, and the pressure p is given by an equation of state, $p = p(\rho, e)$. We restrict ourselves to the ideal gas equation of state, p=$(\gamma - 1)\rho e$.

The integral form of the conservation law is

$$\int_a^b v(x,t_1)\ dx = \int_a^b v(x,t_0)\ dx - \int_{t_0}^{t_1} f(v(b,s))\ ds + \int_{t_0}^{t_1} f(v(a,s))\ ds \tag{1}$$

for any $a < b$ and $0 \le t_0 < t_1$.

The Riemann problem (centered at x_0, t_0) asks for the solution of (1) with initial data

$$v(x,t_0) = \begin{cases} v_l, & x < x_0 \\ v_r, & x > x_0 \end{cases}. \tag{2}$$

The solution is a function of $(x - x_0)/(t - t_0)$,

$$\omega((x - x_0)/(t - t_0)) \tag{3}$$

Godunov's idea for a numerical method to solve the gas dynamic equations for general initial data is first to approximate the initial states by piecewise constant states, then use the solution of the local Riemann problems to construct new piecewise constant states by averaging. Thus, suppose we have a grid with cell centers $x_i = i\Delta x$, $i = 0, \pm 1, \pm 2, \cdots$, cell endpoints $x_{i+1/2} = (i + 1/2)\Delta x$ and discrete time steps $t^n = n\Delta t$. Then given

$$v_i^n = \frac{1}{\Delta x}\int_{x_{i-1/2}}^{x_{i+1/2}} v(x,t^n)\ dx$$

Godunov defines v_i^{n+1} by

$$v_i^{n+1} = \frac{1}{\Delta x}\int_0^{\frac{\Delta x}{2}} \omega_{i-1/2}^n(x/\Delta t)\ dx + \frac{1}{\Delta x}\int_{-\frac{\Delta x}{2}}^0 \omega_{i+1/2}^n(x/\Delta t)\ dx, \tag{4}$$

where $\omega_{i-1/2}^n((x - x_{i-1/2})/(t - t^n))$ is the solution of (2) centered at $(x_{i-1/2}, t^n)$ and with $v_l = v_{i-1}^n$, $v_r = v_i^n$. Since an exact Riemann solution is used, it follows from (1) that there is a numerical flux F such that

$$v_i^{n+1} = v_i^n - \lambda(F_{i+1/2}^n - F_{i-1/2}^n), \tag{5}$$

where

$$F_{i+1/2}^n = f(\omega_{i+1/2}^n(0)), \tag{6}$$

and

$$\lambda = \frac{\Delta t}{\Delta x}. \tag{7}$$

1.2 HLLE

The approximate Riemann solver proposed by Einfeldt [1], based on the HLL solver of Harten, Lax and van Leer [3], and now known as the HLLE solver consists of two speeds and three constant states. Let $x' = x - x_{i+1/2}$, $t^n = 0$, and suppress the index n. Then define

$$\omega_{i+1/2}(x'/t) = \begin{cases} v_i, \ x' < b^l_{i+1/2}t \\ v_{i+1/2}, \ b^l_{i+1/2}t < x' < b^r_{i+1/2}t \\ v_{i+1}, \ x' > b^r_{i+1/2}t \end{cases}, \tag{8}$$

where the left and right speeds $b^l < b^r$ and the intermediate state $v_{i+1/2}$ are to be determined. The speeds are meant to be approximations to the smallest and largest signal velocities of the exact Riemann problem. Einfeldt assumes that

$$\Delta t \max(|b^l|, |b^r|) \leq \Delta x/2. \tag{9}$$

and then defines the intermediate state to satisfy the conservation law, that is,

$$\int_{-\Delta x/2}^{\Delta x/2} \omega_{i+1/2}(x'/t)\ dx = \frac{\Delta x}{2}(v_i + v_{i+1}) - \Delta t(f(v_{i+1}) - f(v_i)),$$

or,

$$v_{i+1/2} = -\frac{f(v_{i+1}) - f(v_i)}{b^r_{i+1/2} - b^l_{i+1/2}} + \frac{b^r_{i+1/2}v_{i+1} - b^l_{i+1/2}v_i}{b^r_{i+1/2} - b^l_{i+1/2}}. \tag{10}$$

The corresponding Godunov scheme is then (5) with

$$F_{i+1/2} = \frac{b^+_{i+1/2}f(v_i) - b^-_{i+1/2}f(v_{i+1})}{b^+_{i+1/2} - b^-_{i+1/2}} + \frac{b^+_{i+1/2}b^-_{i+1/2}}{b^+_{i+1/2} - b^-_{i+1/2}}(v_{i+1} - v_i), \tag{11}$$

where

$$\begin{aligned} b^+_{i+1/2} &= \max(0, b^r_{i+1/2}), \\ b^-_{i+1/2} &= \min(0, b^l_{i+1/2}). \end{aligned} \tag{12}$$

The speeds remain to be chosen. The speeds proposed in [1] are as follows: Let

$$\begin{aligned} H_i &= \frac{1}{\rho_i}(E_i + p_i), \\ c_i &= \sqrt{(\gamma - 1)(H_i - .5u_i^2)}. \end{aligned} \tag{13}$$

Define Roe averages:

$$\begin{aligned} \bar{u}_{i+1/2} &= \frac{\sqrt{\rho_i}u_i + \sqrt{\rho_{i+1}}u_{i+1}}{\sqrt{\rho_i} + \sqrt{\rho_{i+1}}}, \\ \bar{H}_{i+1/2} &= \frac{\sqrt{\rho_i}H_i + \sqrt{\rho_{i+1}}H_{i+1}}{\sqrt{\rho_i} + \sqrt{\rho_{i+1}}}, \\ \bar{c}_{i+1/2} &= \sqrt{(\gamma - 1)(\bar{H}_{i+1/2} - .5\bar{u}^2_{i+1/2})}. \end{aligned}$$

Then the speeds chosen by Einfeldt are

$$\begin{aligned} b^l_{i+1/2} &= \min(\bar{u}_{i+1/2} - \bar{c}_{i+1/2}, u_i - c_i) \\ b^r_{i+1/2} &= \max(\bar{u}_{i+1/2} + \bar{c}_{i+1/2}, u_{i+1} + c_{i+1}). \end{aligned} \tag{14}$$

1.3 Stability, entropy, and positivity

The derivation of the exact and approximate Godunov schemes assumes that waves generated at the cell endpoints do not interact during one time step. In fact, as pointed out in [3], the exact Godunov scheme is valid as long as waves from one endpoint do not reach an adjacent endpoint in one time step. A similar situation holds for the HLLE scheme, in that there is a stability condition derived in [1] that is far less restrictive than (9). It is shown in [5] that both the HLLE scheme with its stability condition and the exact Godunov scheme are positivity-conserving, that is, if the density and internal energy are initially positive then they are for all time. We refer the reader to [3] for a definition and discussion of entropy and the entropy inequality. It is shown there that exact Godunov satisfies the entropy inequality, and that a scheme like HLLE does also if the speeds b^l and b^r bound the exact wave speeds. According to [4] this is not the case for the choice (14), thus, the behavior of entropy for HLLE is unknown.

2 Godunov and HLLE in Two Dimensions

The system of conservation laws is

$$v_t + f_x(v) + g_y(v) = 0,$$

where

$$v = \begin{pmatrix} \rho \\ m \\ n \\ E \end{pmatrix},$$

and

$$f(v) = \begin{pmatrix} m \\ \frac{m^2}{\rho} + p \\ \frac{mn}{\rho} \\ \frac{m}{\rho}(E+p) \end{pmatrix},$$

$$g(v) = \begin{pmatrix} n \\ \frac{mn}{\rho} \\ \frac{n^2}{\rho} + p \\ \frac{n}{\rho}(E+p) \end{pmatrix},$$

where if μ, ν are respectively the x and y components of velocity then $m = \rho\mu$, $n = \rho\nu$, $E = \rho(e + .5(\mu^2 + \nu^2))$, and p and e are pressure and internal energy, as before.

The integral form of the conservation law, specifically for rectangles, is

$$\begin{aligned} \int_a^b \int_c^d v(x,y,t_1)dxdy &= \int_a^b \int_c^d v(x,y,t_0)\, dxdy \\ - \int_{t_0}^{t_1} \int_c^d f(v(b,y,s))\, dyds &+ \int_{t_0}^{t_1} \int_c^d f(v(a,y,s))\, dyds \\ - \int_{t_0}^{t_1} \int_a^b g(v(x,d,s))\, dxds &+ \int_{t_0}^{t_1} \int_a^b g(v(x,c,s))\, dxds \end{aligned} \tag{15}$$

for any $a < b$, $c < d$ and $0 \leq t_0 < t_1$.

There is an infinite variety of two-dimensional Riemann problems, but only one type which is relevant for a rectangular grid, namely, the four quadrant problem (centered at x_0, y_0, t_0), that is, find $v(x, y, t)$ satisfying (15) with initial data

$$v(x, y, t_0) = \begin{cases} v_{ll}, & x < x_0, \ y < y_0 \\ v_{ul}, & x < x_0, \ y > y_0 \\ v_{ur}, & x > x_0, \ y > y_0 \\ v_{lr}, & x > x_0, \ y < y_0 \end{cases} . \tag{16}$$

Unlike the situation in one dimension, where everything is known about the Riemann problem, here almost nothing is known. The complexity of the solution can be seen from the numerical results of [2]. Nevertheless, we can proceed formally and suppose a solution which is a function of $((x - x_0)/(t - t_0), (y - y_0)/(t - t_0))$,

$$\omega((x - x_0)/(t - t_0), (y - y_0)/(t - t_0)). \tag{17}$$

A literal extension of Godunov's idea for a numerical method to solve the gas dynamic equations for general initial data in *two dimensions* is first to approximate the initial states by piecewise constant states, then use the solution of the two-dimensional local Riemann problems to construct new piecewise constant states by averaging. Thus, suppose we have a grid with cell centers $x_i = i\Delta x$, $y_j = j\Delta y$, $i, j = 0, \pm 1, \pm 2, \cdots$, cell vertices $x_{i+1/2} = (i + 1/2)\Delta x$, $y_{j+1/2} = (j + 1/2)\Delta y$ and discrete time steps $t^n = n\Delta t$. Then given

$$v_{i,j}^n = \frac{1}{\Delta x \Delta y} \int_{x_{i-1/2}}^{x_{i+1/2}} \int_{y_{j-1/2}}^{y_{j+1/2}} v(x, y, t^n) \ dydx$$

we could define $v_{i,j}^{n+1}$ by

$$\begin{aligned} v_{i,j}^{n+1} = & \frac{1}{\Delta x \Delta y} \int_0^{\frac{\Delta x}{2}} \int_0^{\frac{\Delta y}{2}} \omega_{i-1/2,j-1/2}^n(x/\Delta t, y/\Delta t) \ dydx \\ & + \frac{1}{\Delta x \Delta y} \int_0^{\frac{\Delta x}{2}} \int_{-\frac{\Delta y}{2}}^0 \omega_{i-1/2,j+1/2}^n(x/\Delta t, y/\Delta t) \ dydx \\ & + \frac{1}{\Delta x \Delta y} \int_{-\frac{\Delta x}{2}}^0 \int_{-\frac{\Delta y}{2}}^0 \omega_{i+1/2,j+1/2}^n(x/\Delta t, y/\Delta t) \ dydx \\ & + \frac{1}{\Delta x \Delta y} \int_{-\frac{\Delta x}{2}}^0 \int_0^{\frac{\Delta y}{2}} \omega_{i+1/2,j-1/2}^n(x/\Delta t, y/\Delta t) \ dydx \end{aligned} \tag{18}$$

where $\omega_{i-1/2,j-1/2}^n((x - x_{i-1/2})/(t - t^n), (y - y_{j-1/2})/(t - t^n))$ is the solution of (16) centered at $(x_{i-1/2}, y_{j-1/2}, t^n)$ and with $v_{ll} = v_{i-1,j-1}^n$, $v_{ul} = v_{i-1,j}^n$, $v_{ur} = v_{i,j}^n$, $v_{lr} = v_{i,j-1}^n$.

This construction only makes sense if waves generated at the cell vertices by the 2D Riemann problems do not interact with each other. So if σ is the maximum signal speed, maximized over all directions and all vertices, then we require $\sigma \Delta t < \min(\Delta x/2, \Delta y/2)$.

2.1 The nine-state Riemann solver

Unfortunately, the above is all fantasy since there is no possibility of solving (16) exactly. So let us consider what an approximate solution might look like in Fig. 1. It depicts a box centered at

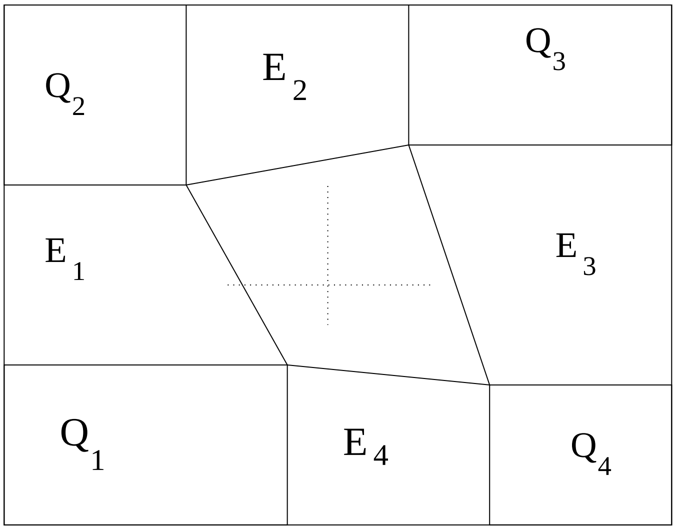

Figure 1: Structure of the 2D solution at later time. Dotted lines indicate initial center of the Riemann problem

.

the Riemann problem center, with horizontal and vertical sides of length Δx and Δy respectively, at some fixed small time after the evolution of the solution has begun. Then, because signals propagate with finite speed we can define nine regions with the following properties: The corner regions Q_i are taken to be rectangles in which the data is unchanged from its initial values. In the edge strips E_i the state is determined by the one-dimensional Riemann problems formed by the states on either side of the appropriate axis. The remaining central region contains the two-dimensional interaction.

In analogy with the one-dimensional case, our two-dimensional HLLE solution assigns a constant state to each of the nine regions. The four corner rectangles have their initial values. In the edge strips the constant state will be the intermediate state obtained from the one-dimensional HLLE solver. Then (15) will be used to define the central constant state.

Consider the cell vertex $(x_{i+1/2}, y_{j+1/2})$. The four states interacting at this vertex are (suppressing the time index) $v_{i,j},\ v_{i+1,j},\ v_{i+1.j+1},\ v_{i,j+1}$. Let us first define the interior vertex P_k of each Q_k in Fig. 1. These will be determined by four speeds which will in turn be defined by one-dimensional HLLE speeds. So, let

$$\begin{aligned}
b^{ul}_{i+1/2,j+1/2} &= (b^{l}_{i+1/2,j+1}, b^{r}_{i,j+1/2}),\\
b^{ur}_{i+1/2,j+1/2} &= (b^{r}_{i+1/2,j+1}, b^{r}_{i+1,j+1/2}),\\
b^{lr}_{i+1/2,j+1/2} &= (b^{r}_{i+1/2,j}, b^{l}_{i+1,j+1/2}),\\
b^{ll}_{i+1/2,j+1/2} &= (b^{l}_{i+1/2,j}, b^{l}_{i,j+1/2}).
\end{aligned} \tag{19}$$

(See the appendix for the detailed definition of these speeds). For example, $b^{l}_{i+1/2,j+1}$ and $b^{r}_{i+1/2,j+1}$ are the left and right HLLE speeds for the one-dimensional Riemann problem in the x-direction (with flux f) with $v_l = v_{i,j+1}$ and $v_r = v_{i+1,j+1}$, while $b^{l}_{i,j+1/2}$ and $b^{r}_{i,j+1/2}$ are the left and right HLLE speeds for the one-dimensional Riemann problem in the y-direction (with flux g) with $v_l = v_{i,j}$ and $v_r = v_{i,j+1}$.

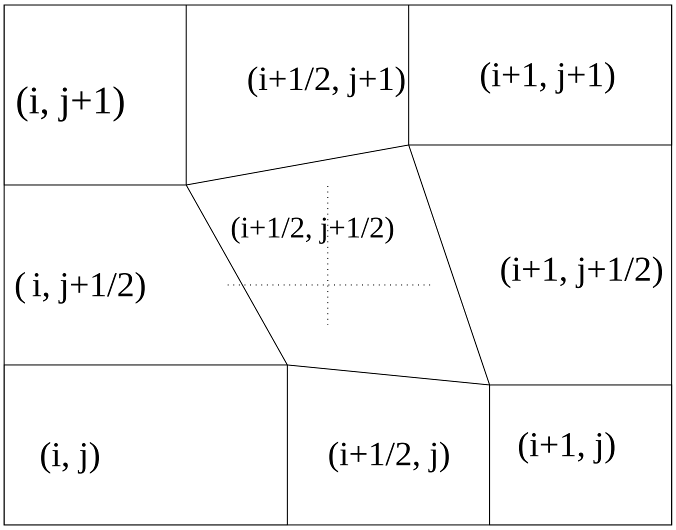

Figure 2: Indexing of the nine regions

.

Now, let P_k be the interior vertex of Q_k, and rename them $P_1 = P^{ll}$, $P_2 = P^{ul}$, $P_3 = P^{ur}$, $P_4 = P^{lr}$, where

$$\begin{aligned}
P^{ll}(t) &= (x_{i+1/2}, y_{j+1/2}) + b^{ll}_{i+1/2,j+1/2}(t - t^n), \\
P^{ul}(t) &= (x_{i+1/2}, y_{j+1/2}) + b^{ul}_{i+1/2,j+1/2}(t - t^n), \\
P^{ur}(t) &= (x_{i+1/2}, y_{j+1/2}) + b^{ur}_{i+1/2,j+1/2}(t - t^n), \\
P^{lr}(t) &= (x_{i+1/2}, y_{j+1/2}) + b^{lr}_{i+1/2,j+1/2}(t - t^n).
\end{aligned}$$

However,since it is possible that $b^l > 0$ or $b^r < 0$, the corner rectangles might not be contained in their respective quadrants, as they are in Fig. 1. If that happens the picture might in some cases not be as simple as shown and the computer code would have to be quite complicated in order to allow for this situation. This difficulty can be avoided at the cost of introducing somewhat more diffusion than is present in the 1D HLLE method. What is needed is to use (12) and replace (19) with

$$\begin{aligned}
b^{ul}_{i+1/2,j+1/2} &= (b^-_{i+1/2,j+1}, b^+_{i,j+1/2}), \\
b^{ur}_{i+1/2,j+1/2} &= (b^+_{i+1/2,j+1}, b^+_{i+1,j+1/2}), \\
b^{lr}_{i+1/2,j+1/2} &= (b^+_{i+1/2,j}, b^-_{i+1,j+1/2}), \\
b^{ll}_{i+1/2,j+1/2} &= (b^-_{i+1/2,j}, b^-_{i,j+1/2}).
\end{aligned} \tag{20}$$

Referring to Fig. 2 we can now define the edge states $v_{i,j+1/2}$, $v_{i+1/2,j}$, $v_{i+1,j+1/2}$, and $v_{i+1/2,j}$. For example, $v_{i,j+1/2}$ is the HLLE intermediate state for the Riemann problem in the y-direction with $v_l = v_{i,j}$ and $v_r = v_{i,j+1}$, and the others are defined similarly.

We can state the complete solution. Let $S_{i+\alpha,j+\beta}$ for $\alpha = 0, 1/2, 1$, $\beta = 0, 1/2, 1$ be the nine regions. Then

$$\omega_{i+1/2,j+1/2}(x, y) = v_{i+\alpha,j+\beta} \text{ for } (\mathrm{x}, \mathrm{y}) \in \mathrm{S}_{\mathrm{i}+\alpha,\mathrm{j}+\beta}. \tag{21}$$

The ninth state $v_{i+1/2,j+1/2}$ is yet to be defined. Let $A_{i+\alpha,j+\beta}$ be the area of $S_{i+\alpha,j+\beta}$ at time $t = t^{n+1}$. Then based on (15) we can write the following approximate integral conservation form:

$$
\begin{aligned}
\sum_{\substack{\alpha = 0, 1/2, 1\\ \beta = 0, 1/2, 1}} A_{i+\alpha,j+\beta} v_{i+\alpha,j+\beta} &= \frac{\Delta x \Delta y}{4} \sum_{\substack{\alpha = 0, 1\\ \beta = 0, 1}} v_{i+\alpha,j+\beta} \\
&- \Delta y \Delta t (F_{i+1,j+1/2} - F_{i,j+1/2}) \\
&- \Delta x \Delta t (G_{i+1/2,j+1} - G_{i+1/2,j}),
\end{aligned} \tag{22}
$$

from which $v_{i+1/2,j+1/2}$ can be obtained if $A_{i+1/2,j+1/2} \neq 0$. The flux integrals will also be approximated using the 1D HLLE solutions. Note that (15) is being formulated over the space-time cell $C = \{x, y, t;\ x_i \leq x \leq x_{i+1},\ y_j \leq y \leq y_{j+1},\ t^n \leq t \leq t^{n+1}\}$. The flux integrals are integrals over the time-like faces of this cell. For example, consider the face $x = x_i$, shown in Fig. 3. For it we have

$$
\begin{aligned}
F_{i,j+1/2} &= \frac{1}{\Delta t \Delta y}[\frac{1}{2}(\Delta y - b^r_{i,j+1/2}\Delta t)\Delta t f(v_{i,j+1}) \\
&+ \frac{1}{2}(\Delta y + b^l_{i,j+1/2}\Delta t)\Delta t f(v_{i,j}) \\
&+ \frac{1}{2}(b^r_{i,j+1/2} - b^l_{i,j+1/2})(\Delta t)^2 f(v_{i,j+1/2})].
\end{aligned} \tag{23}
$$

In the same way,

$$
\begin{aligned}
G_{i+1/2,j} &= \frac{1}{\Delta t \Delta x}[\frac{1}{2}(\Delta x - b^r_{i+1/2,j}\Delta t)\Delta t g(v_{i+1,j}) \\
&+ \frac{1}{2}(\Delta x + b^l_{i+1/2,j}\Delta t)\Delta t g(v_{i,j}) \\
&+ \frac{1}{2}(b^r_{i+1/2,j} - b^l_{i+1/2,j})(\Delta t)^2 g(v_{i+1/2,j})].
\end{aligned} \tag{24}
$$

2.2 The 2D HLLE-Godunov scheme

Just as with 1D, we use the approximate Riemann solution in place of the exact one. There are two phases to the computation.

PHASE 1.

Call the $\Delta x \times \Delta y$ cells centered on the vertices the *dual* cells, and call the original cells the *primary cells*. For each dual cell edge store the pair of speeds, the 1D intermediate state, and the fluxes F and G.

PHASE 2.

For each dual cell define the nine pieces, compute their areas, and then find the central intermediate state. Substitute the approximation given by (21) into (18) to obtain new constant states in the primary cells. This is quite easy since with (20) the corner rectangles Q_i in Fig. 1 lie entirely in their respective quadrants. Each edge set is a trapezoid which now splits into two trapezoids, each lying entirely in a quadrant. The area of the intersection of the central region with a quadrant is simply what is left over from the other three pieces. So the mapping onto the primary cells can be accomplished without a separate pass over the primary cells, by accumulating the contribution of each dual cell to its neighboring primary cells.

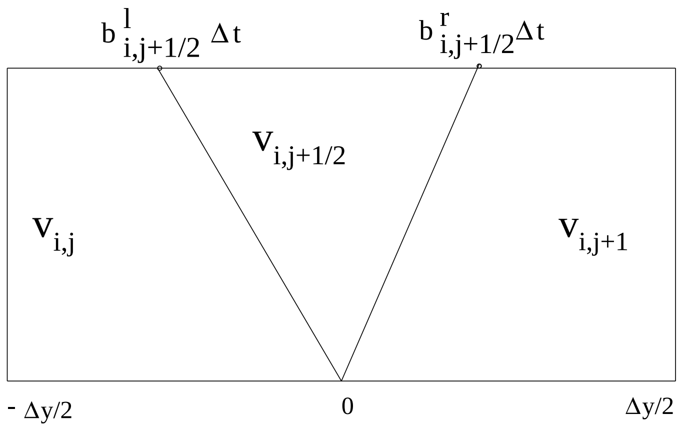

Figure 3: Face $x = x_i$

.

2.3 Stability, entropy, and positivity

There is little that can be said at this time about these difficult issues for the 2D HLLE scheme, for several reasons. The computer program performing the operations described in section 2.2 is fairly simple, but the formula describing the finite difference scheme in terms of the speeds and the hydrodynamic states is very complicated, making an analysis of stability or positivity extremely difficult. If we were using *exact* Riemann solvers for the 1D problems, *exact* integrals for the face fluxes and average intermediate states, and if the central region were *guaranteed* to contain all the 2D interactions, the convexity argument of [3] could presumably be used to establish an entropy inequality. Since none of these is the case, we are much worse off here concerning entropy than in 1D.

For the numerical examples we used an adaptive time step determined by

$$\max(\lambda_x \sigma_x, \lambda_y \sigma_y) \leq \text{CFL} \leq 1,$$

where $\lambda_x = \Delta t/\Delta x$, $\lambda_y = \Delta t/\Delta y$, and σ_x, σ_y are the wave speeds in each direction. The maximum is taken over the grid as well as over the pair.

3 Numerical examples

We computed cases 3 and 4 of [2], using a grid 400 × 400, shown in Figs. 4 and 5. For comparison we show the same result for the composite scheme CFLF4, developed in [6], for case 4, and CFLF8 for case 3. All computations were done with CFL=.9. Surprisingly, CFLF4 is only about 9% faster than HLLE. For case 4 all the left speeds b^l were negative and all the right speeds b^r were positive, but for case 3 some left speeds were positive.

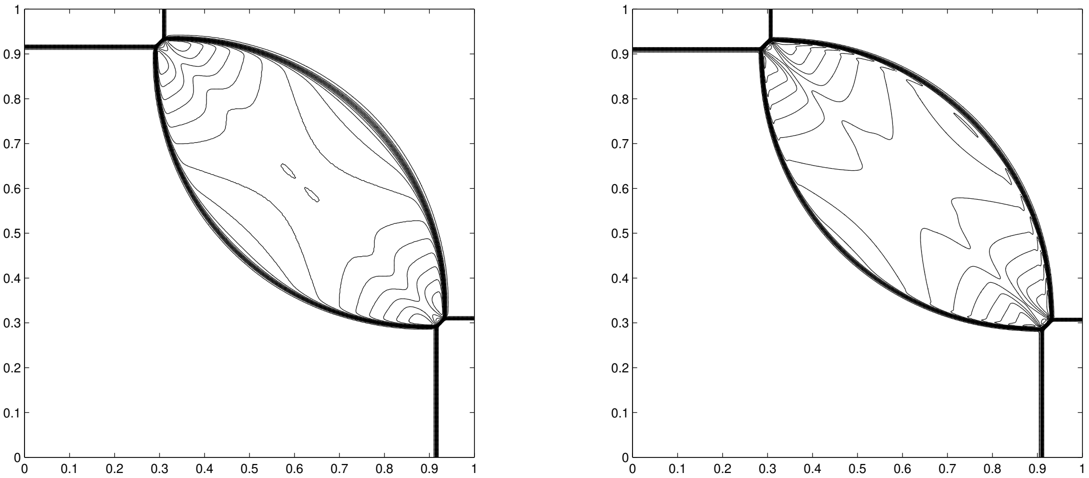

a) b)

Figure 4: Configuration 4. 400 $\times$ 400 grid, time=.25, cfl=.9, 30 contours: a) 2D HLLE. b) CFLF4
.

4 Appendix: 2D Einfeldt speeds

Multi-dimensional Roe averages are given in [7]. They are as follows: Let

$$\begin{aligned} H_{i,j} &= \frac{1}{\rho_{i,j}}(E_{i,j}+p_{i,j}), \\ c_{i,j} &= \sqrt{(\gamma-1)(H_{i,j}-.5(\mu_{i,j}^2+\nu_{i,j}^2))}. \end{aligned}$$

Then

$$\begin{aligned} \bar{\mu}_{i+1/2,j} &= \frac{\sqrt{\rho_{i,j}}\mu_{i,j}+\sqrt{\rho_{i+1,j}}\mu_{i+1,j}}{\sqrt{\rho_{i,j}}+\sqrt{\rho_{i+1,j}}}, \\ \bar{\nu}_{i+1/2,j} &= \frac{\sqrt{\rho_{i,j}}\nu_{i,j}+\sqrt{\rho_{i+1,j}}\nu_{i+1,j}}{\sqrt{\rho_{i,j}}+\sqrt{\rho_{i+1,j}}}, \\ \bar{H}_{i+1/2,j} &= \frac{\sqrt{\rho_{i,j}}H_{i,j}+\sqrt{\rho_{i+1,j}}H_{i+1,j}}{\sqrt{\rho_{i,j}}+\sqrt{\rho_{i+1,j}}}, \\ \bar{c}_{i+1/2,j} &= \sqrt{(\gamma-1)(\bar{H}_{i+1/2,j}-.5(\bar{\mu}_{i+1/2,j}^2+\bar{\nu}_{i+1/2,j}^2))}. \end{aligned}$$

Then define the speeds:

$$\begin{aligned} b_{i+1/2,j}^r &= \max(\bar{\mu}_{i+1/2,j}+\bar{c}_{i+1/2,j}, \mu_{i+1,j}+c_{i+1,j}) \\ b_{i+1/2,j}^l &= \min(\bar{\mu}_{i+1/2,j}-\bar{c}_{i+1/2,j}, \mu_{i,j}-c_{i,j}). \end{aligned}$$

The speeds $b_{i,j+1/2}^r$, $b_{i,j+1/2}^l$ are obtained by interchanging the indices in all the doubly indexed quantities above, then interchanging i and j and then interchanging μ and ν.

References

[1] B. Einfeldt, On Godunov-type methods for gas dynamics, *SIAM J. Numer. Anal.* **25**, 294-318 (1988).

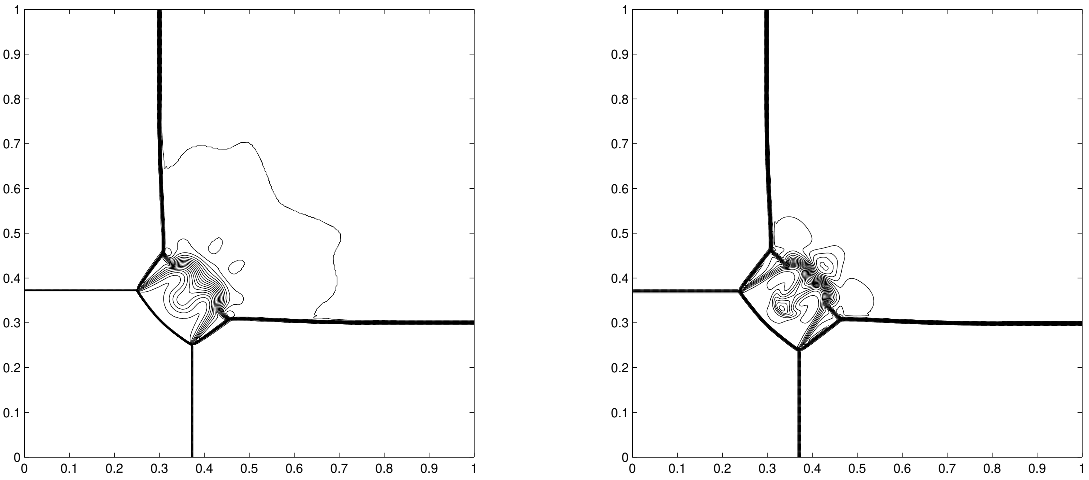

a) b)

Figure 5: Configuration 3. 400 $\times$ 400 grid, time=.3, cfl=.9, 30 contours: a) 2D HLLE. b) CFLF4
.

[2] C. W. Schulz-Rinne, J. P. Collins, and H. M. Glaz, Numerical solution of the Riemann problem for two-dimensional gas dynamics, *SIAM J. Sci. Comput.* **14**, 1394–1414 (1993).

[3] A. Harten, P. D. Lax and B. van Leer, On upstream differencing and Godunov-type schemes for hyperbolic conservation laws, *SIAM Rev.* **25**, 35-61 (1983).

[4] P. Batten, N. Clarke, C. Lambert, and D. M. Clauson, On the choice of wavespeeds for the HLLC Riemann solver, *SIAM J. Sci. Comput.* **18** , 1553-1570 (1997).

[5] B. Einfeldt, C. D. Munz, P. L. Roe, and B. Sjøgreen, On Godunov-type methods near low densities, *J. Comp. Phys.* **92**, 273-295 (1991).

[6] R. Liska and B. Wendroff, Composite schemes for conservation laws, *SIAM J. Numer. Anal.* **35**, 2250-2271 (1998).

[7] E. F. Toro, Riemann Solvers and Numerical Methods for Fluid Dynamics, Springer, 1997